Emerald Aircraft Engineering and Aerospace Technology: An International Journal

Implicit CFD Methods for Transitional Shock Wave – Boundary Layer Interaction

Journal:	*Aircraft Engineering and Aerospace Technology*
Manuscript ID	AEAT-05-2015-0123.R1
Manuscript Type:	Research Paper
Keywords:	Buffet, Transition, CFD

Implicit CFD Methods for Transitional Shock Wave – Boundary Layer Interaction

Abstract

In this paper, the potential of transition prediction methods is explored for modelling transitional shock-wave/boundary-layer interactions. The study is fuelled by the strong interest of researchers and airframe manufacturers in reducing drag of vehicles flying at transonic speeds. The principle of drag reduction via flow laminarity is valid, provided there is no need for the flow to sustain large pressure gradients or shocks. This is true since laminar boundary layers are less resistant to flow separation. It is therefore worthwhile to assess the performance of CFD methods in modelling laminar boundary layers that can be tripped to turbulent just before the interaction with a shock. At this work, the CFD solver of Liverpool University is used. The method is strongly implicit and for this reason the implementation of 4-equation, intermittency-based models requires special attention. The Navier-Stokes equations, the transport equations of the kinetic energy of turbulence (κ) and the turbulent frequency (ω) are inverted at the same time as the transport equations for the flow intermittency (γ) and the momentum thickness Reynolds number ($Re_{\theta tr}$). The result is stable and robust convergence even for complex 3D flow cases. The method is demonstrated for the flow around the V2C section of the TFAST EU, F7 project. The results suggest that the intermittency based model captures the fundamental physics of the interaction but verification and validation is needed to ensure that accurate results can be obtained. For this reason, comparisons with the TFAST experiments is put forward as a means of establishing confidence in the transition prediction tools employed for shock/boundary-layer interaction simulation.

Keywords Intermittency-based models; CFD; shock boundary interaction; flow transition.

Paper type Research paper.

Introduction

Engineers face complex challenges during the design of civil aircraft, in their efforts to achieve low fuel consumption at cruise conditions where the Mach number ranges from 0.7 to 0.9. At these conditions, the formation of shocks on the wing can lead in increased drag or even more unfavourable conditions like buffet.

At transonic speeds, the challenges for CFD come mainly from shock wave/boundary layer interaction (SWBLI). In

general, inaccurate predictions of shock waves have large impact on the global aerodynamics coefficients. The proper computation of the shock-wave location depends on the accurate prediction of turbulence boundary layers, whose properties are in turn influenced by shock waves. The situation becomes more complicated when a shock is sufficiently strong to cause flow separation, which often gives rise to an unsteady SWBLI commonly known as transonic buffet. In this case, the shock wave oscillates in a large-amplitude motion, producing strong fluctuations of aerodynamics forces and moments.

Buffet can adversely affect the performance and stability of the aircraft. The phenomenon is characterized by a shock oscillation and unsteady shock wave-boundary layer interaction. Because of the movement of the shock, pressure waves are formed, and propagate downstream in the separated flow region. Disturbances from the trailing edge are also interacting with the shock and help to maintain its oscillation.

Tijdeman and Seebass (1980) classified the shock wave motions by the oscillation amplitude as: Type A, for small amplitude near-sinuous streamwise oscillations; Type B, characterized by an large amplitude streamwise oscillation but with an interruption of the shock motion and, Type C, where high amplitude oscillations are observed with the main wave structure changing from compression waves to shock waves and then weak compression waves.

The first attempt to numerically investigate the transonic buffet was in work of Levy *et al* (1978). Levy reproduced the work of McDevitt *at al* (1976) on a symmetric circular-arc aerofoil over three different Mach numbers using two-dimensional RANS computations in conjunction with an algebraic eddy-viscosity turbulence model. The simulations showed good agreement with the experimental data for the mean pressure distribution. Although, the shock location was predicted far downstream and large differences were found near the aft part of the aerofoil.

Seegmiller *et al* (1978) used the same algebraic model as Levy to investigate the unsteady periodic flow over the circular-arc aerofoil at M_{∞} of 0.76 and Re of 11×10^6. The simulations showed that the shock was formed near the trailing edge and as the shock moved upstream, a large-scale vortex shedding could be observed beyond the trailing edge.

Lee (2001) presented a comprehensive review of shock-buffet studies, including physical models of the shock-buffet mechanism. These mechanisms were discussed for symmetrical circular-arc aerofoils at zero incidences and for supercritical aerofoils at high incidence angles with fully separated flows. During the examinations, Lee suggested that the buffet period is equal to the sum of the downstream and upstream wave's motion time. Those pressure waves are produced either from the shock wave moving downstream to the trailing edge or the trailing edge boundary layer and move upstream towards the shock. Estimating these motions by empirical evaluation over a single buffet cycle, Lee obtained good agreement with experiments.

Figure 1 Self-excited shock wave oscillation model on aerofoil (Lee, 2001).

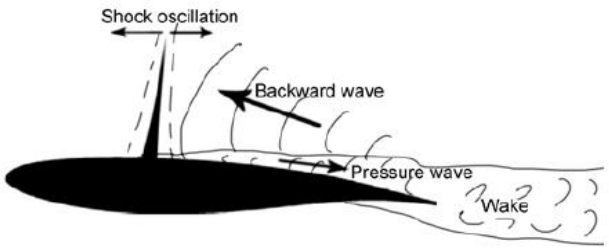

Numerical investigations for the transonic flow over the NASA 18% thick circular-arc aerofoil at M_{∞} of 0.76 and Re of $11x10^6$ were also provided by Marvin *et al* (1980). Although, the unsteady flow features were well reproduced, they appeared later in the buffet period compared to the experiments. For a given streamwise station, the velocities before the shock were higher than the experimental data. Marvin concluded that an algebraic turbulence model developed for steady flows could only qualitatively reproduce the features of the unsteady flow.

Besides the numerical method, the turbulence model is a major source of uncertainties in the simulation of transonic buffet. Several studies used CFD solutions to investigate the shock-buffet phenomenon (Barakos and Drikakis, 2000; Deck, 2005; Boin *et al.*, 2006; Raveh, 2009; Iovnovich, 2011, Grossi *et al.*, 2011). During their study, Barakos and Drikakis (2000) assessed a range of turbulence models against the experimental data of McDevitt and Okuno (1985) concerning the buffet boundaries of a NACA0012 aerofoil. They tested difference classes of turbulence closures including algebraic Baldwin-Lomax model, the one equation Spalart-Allmaras model and the linear low-Reynolds two-equation κ-ε and κ-ω models. Using these models, the buffet boundary as a function of Mach number and angle of attack was determined. In general, the trailing edge buffet onset appeared at incidences higher than what suggested by the experiments and this could be due to the absence of the wind tunnel wall effects in the calculations. Using a two-dimensional approach, Thiery and Coustols (2009), demonstrated that the modelling of the wind tunnel walls should not be determinant for the evaluation of the capability of a turbulent model in predicting the shock wave motion in their OAT15A case. A recent study by Iovnovich and Raveh (2014) presented a computational study of the transonic shock wave/boundary layer interaction phenomenon on three-dimensional wings. Using similar flow conditions to the two-dimensional simulations, they compared the buffet characteristics and suggested a connection between them.

The previous studies have shown the challenge that can be the shock-wave/boundary layer interaction for the turbulence modelling. A challenge that can be affected by the accurate prediction of the laminar-turbulent transition of boundary layer. Transition prediction is among the most challenging and important problem in flow modelling within implications in every application domain. The variety of possible transition mechanisms makes it difficult to propose a general modelling strategy. Based on the above, the objective of this paper is to show the effect of transition location on the structure of Shock Wave Boundary Layer interaction (SWBLI). Emphasis is placed on how close the induced transition may be to the

shock wave while still maintaining a turbulent character of interaction.

CFD Solver

The Helicopter Multi-Block solver of Liverpool (HMB2) is the main CFD tool employed for this work. This code offers an efficient algorithm for solving the Navier-Stokes (NS) equations along with transport equations of one and two-equation turbulence models and assesses several transition prediction models. The unsteady Navier-Stokes equations are discretising on a curvilinear, multi-block, body conforming mesh using a cell-centred finite volume method. The computational domain is divided into a finite number of non-overlapping control volumes, and the governing equations are applied to each cell in turn. The spatial discretization of the NS equations leads to a set of ordinary differential equations in time

$$\frac{d}{dt}(W_{i,j,k}V_{i,j,k}) = -R_{i,j,k}(W) \tag{1}$$

where i , j , k represent spatial components. W and R are the vectors of the cell conserved variables and residuals, respectively.

The implicit dual-time method proposed by Jameson (1991) is used for time-accurate calculations. The residual is redefined to obtain a steady state equation, which can be solved using acceleration techniques. The following system of equations are solved in the implicit scheme during the dual-time integration process:

$$\frac{\mathrm{D}VW_{i,j,k}^{m+1} - \mathrm{D}VW_{i,j,k}^{m}}{\mathrm{D}V\mathrm{D}t} + \frac{\mathrm{D}VW_{i,j,k}^{n+1} - \mathrm{D}VW_{i,j,k}^{n}}{\mathrm{D}V\mathrm{D}t} = R_{i,j,k}^{n+1} \tag{2}$$

where ΔV is the change in cell volume, $\mathrm{D}t$ is the pseudo time-step increment and $\mathrm{D}t$ is the real time-step increment.

The flux residual is approximately defined by:

$$R_{i,j,k}^{n+1} \approx R_{i,j,k}^{n+1} + \frac{\partial R_{i,j,k}^{n}}{\partial W_{i,j,k}^{n}}(W_{i,j,k}^{n+1} - W_{i,j,k}^{n}) \tag{3}$$

By substituting equation 3 into equation 2, the resulting linear system can be written as:

$$\left(\frac{1}{\mathrm{D}t} + \left(\frac{\partial R}{\partial W}\right)^{n}\right)\mathrm{D}W = -R^{n} \tag{4}$$

where the subscripts i , j , k have been dropped for clarity and ΔW is used for $\left(W_{i,j,k}^{n+1} - W_{i,j,k}^{n}\right)$.

The above equations must be solved for each cell of the mesh and provide an update to the vector of variables ΔW . The assembly of the discrete equations over the computational domain results in a system of equations in the form of $Ax = b$ with extra complexity. To compute the linear system efficiently in terms of time and memory, the iterative method of Conjugate Gradient (CG) is used. The CG method finds an approximation to the solution by minimizing a suitable residual

error function in a finite dimensional space of potential solution vectors. A Generalised Conjugated Gradient (GCG) (Axelsson, 1994) method is then used in conjunction with a Block Incomplete Lower-Upper (BILU) (Axelsson, 1994) factorisation as a pre-conditioner to solve the linear system of equations, which is obtained from a linearization in pseudo-time. The BILU factorisation is decoupled between blocks on different processors to improve parallel efficiency. This approach does not seem to have a major impact on the solution as the number of blocks increases. During the calculations, a specified number of Euler iterations are executed before switching to the implicit scheme.

For a block-structured mesh, the linear system, shown in equation 4, represents a large, sparse matrix, which arises from the implicit discretisation in pseudo time. The derived Jacobean matrix is calculated analytically by repeated application of the chain rule. The residual for one cell is built up as a summation of the fluxes through the cell faces. The result of the above is the Jacobian matrix which appears in the left hand side of the discretization and has a number of non-zero entries per row. With the use of the GCG method, the linear system is easier to solve since approximate Jacobian matrices can be used that are more diagonally dominant. All equations are solved simultaneously for the next time level which allows flexibility if the cross-terms are added to the Jacobian matrix. Advantages of this formulation are the lower memory requirements as long as the lower required CPU-time. Solving the Navier-Stokes equations augmented with the transport equations of turbulence and transition models results to a Jacobian matrix with given sparsity pattern. For one and two equation turbulence models, the block structure is given by:

$$\begin{bmatrix} B_{00} & B_{01} \\ B_{10} & B_{11} \end{bmatrix}$$

The B_{00} is a 5x5 matrix and is associated with the flow variable ρ, u, v, w and p. The B_{11} is either a scalar for a one-equation turbulence model or a 2x2 matrix for a two-equation model. The term B_{01} is related to how the fluid variables depend on the turbulent variables while block B_{10} describes how the turbulent variables depend on the fluid variables. Otherwise, one or both blocks can be considered zero and drive to more sparse system. In the case of a transition model is in use, an extra row is added. The matrix is given by:

$$\begin{bmatrix} B_{00} & B_{01} & B_{02} \\ B_{10} & B_{11} & B_{12} \\ B_{20} & B_{21} & B_{22} \end{bmatrix}$$

here the first row is associated with the fluid variables ρ , u, v, w , p, the second row is related to the turbulent model, κ-ω , while the last row is related to the LCTM model.

On each processor, a vector is allocated that contains all the halo cells for all grid blocks. Sending a series of messages between the respective processes performs inter-process communication, each corresponding to a block connection, containing the halo cell data. The messages are sent in chunks of 10,000 double precision numbers using non-blocking

send and receive MPI function. The solver includes a range of one- and two-equation turbulence models, Smagorinsky-based LES, and SAS/DES/IDDES model (Menter, 2005; Shur et al, 1999).

Transition Modelling

A common empirical transition correlation is Michel's criterion (1951). This model predicts the transition location due to the growth of Tollmien-Schlichting instabilities. Based on this criterion, the onset of the transition is assumed to occur where the local Reynolds number, based upon the momentum thickness of the boundary layer, exceeds a critical value determined by the following equation:

$$\mathrm{Re}_{\theta,tr} = 2.9\,\mathrm{Re}_{x,tr}^{0.4} \tag{5}$$

in which the $\mathrm{Re}_{\theta,tr}$ and $\mathrm{Re}_{x,tr}$ are the local Reynolds numbers based on the momentum thickness and on the aerofoil distance from the leading edge, respectively.

Based on Michel's criterion, Cebeci and Smith (1974) suggested an improved correlation to predict the onset of transition given by the following equation:

$$\mathrm{Re}_{\theta,tr} = 1.174\left(1+\frac{22400}{\mathrm{Re}_{x,tr}}\right)\mathrm{Re}_{x,tr}^{0.46} \tag{6}$$

As experimental results for the onset of transition were made available, Abu-Ghannam and Shaw (1980) tried to estimate the experimental results for the zero pressure gradient experiments on flat plates with a line. They proposed a modification to the Hall and Gibbing's relationship (1980) and the momentum thickness Reynolds number at the start of transition was related with the pressure gradient parameter (λ_θ) and the turbulence levels (*Tu*). Abu-Ghannam and Shaw's correlation is written in the following form:

$$\mathrm{Re}_{q,s} = 163 + e^{\{F(\lambda_q) - \frac{F(\lambda_q)}{6.91}Tu\}} \tag{7}$$

where the function F is based on the pressure gradient parameter, and was derived to fit the experimental data.

Besides the prediction for the onset of the transitional region, Abu-Ghannam and Shaw proposed a relation for the end of the transitional flow. This relation relates the local Reynolds number at the end of transition with the Reynolds number at the onset of this mechanism by

$$\mathrm{Re}_{q,e} = \mathrm{Re}_{q,s} + 16.8(\mathrm{Re}_{q,s})^{0.8} \tag{8}$$

Another approach to estimate the onset of transition is the use of transport equations. These models are linked with the calculation of intermittency (the probability of the flow being turbulent at some point). Dhawan and Narasihma (1958) developed an algebraic equation to describe the link between the generation of turbulent spots observed during a transitional flow and the streamwise evolution of the intermittency factor. Steeland and Dick (1996), following the

correlation for the intermittency factor of Dhawan and Narasihma, developed an intermittency transport model for flows in gas turbines. A number of researchers (Cho et al, 1992; Suzen et al, 1999) worked on the idea of intermittency transport equations, especially in the area of turbomachinery. Although, these models have similar structure with the equations used in the turbulent models, are based on non-local formulations requiring information of the flow outside the boundary layer.

In 2006, Menter *et al.* (2006) proposed a transport-equation model based only on local information, which was called γ-$Re_{\theta t}$ model. The transition model of consists of two transport equations: the equation for the intermittency, g, and the equation for the transition momentum thickness Reynolds number, $Re_{\theta t}$, which is formulated in terms of the scalar quantity, $Re_{\theta t}$. The γ-equation is used to trigger the transition process and the $Re_{\theta t}$- equation is employed to avoid the use of non-local variables.

Both transport equations are written as:

$$\frac{\partial(\rho\gamma)}{\partial t}+\frac{\partial(\rho u_j\gamma)}{\partial x_j}=P_{\gamma 1}+P_{\gamma 2}+\frac{\partial}{\partial x_j}\left[\left(\mu+\frac{\mu_t}{\sigma_f}\right)\frac{\partial\gamma}{\partial x_j}\right] \tag{9}$$

$$\frac{\partial(\rho\tilde{\mathrm{Re}}_{\theta t})}{\partial t}+\frac{\partial(\rho u_j\tilde{\mathrm{Re}}_{\theta t})}{\partial x_j}=P_\theta+\frac{\partial}{\partial x_j}\left[(\mu+\mu_t)\frac{\partial\tilde{\mathrm{Re}}_{\theta t}}{\partial x_j}\right] \tag{10}$$

Although the model is considered as correlation-free transition model, a number of empirical equations are used and they are identified as functions of the scalar transition momentum thickness Reynolds number. The first one refers to the critical Reynolds number where the intermittency begins to increase in the boundary layer. This occurs upstream of the transition Reynolds number and is defined as follows:

$$\mathrm{Re}_{\theta c}=\tilde{\mathrm{Re}}_{\theta t}-396.035\cdot10^{-2}+(-120.656\cdot10^{-4})\tilde{\mathrm{Re}}_{\theta t}+(868.23\cdot10^{-6})\tilde{\mathrm{Re}}_{\theta t}+(-696.506\cdot10^{-9})\tilde{\mathrm{Re}}_{\theta t}\quad \text{if } \tilde{\mathrm{Re}}_{\theta t}\le 1870$$

$$=\tilde{\mathrm{Re}}_{\theta t}-(593.11+0.482\cdot(\tilde{\mathrm{Re}}_{\theta t}-1870))\quad \text{if } \tilde{\mathrm{Re}}_{\theta t}\ge 1870 \tag{11}$$

The scalar quantity from the transport equation is forced to match the local value of $Re_{\theta t}$, which is related to the local turbulence intensity and the pressure gradient parameter, and is given by the following empirical equation:

$$\mathrm{Re}_{\theta t}=(1173.51-589.428Tu+\frac{0.2196}{Tu^2}F(\lambda_\theta)\quad \text{if } Tu\le 1.3$$

$$=331.5(Tu-0.5658)^{-0.671}F(\lambda_\theta)\quad \text{if } Tu>1.3 \tag{12}$$

The last correlation describes the length of the transition model and is based on the European Research Community on Flow Turbulence and Combustion (ERCOFTAC) T3 series of flat plate experiments (Savill, 1993). The empirical correlation for the F_{length} is based on $Re_{\theta t}$ and given by:

$$F_{length} = 39.8189 - (119.27 \cdot 10^{-4})\,\tilde{\mathrm{Re}}_{\theta t} - (132.567 \cdot 10^{-6})\,\tilde{\mathrm{Re}}_{\theta t}^{2} \quad \text{if } \tilde{\mathrm{Re}}_{\theta t} \le 400$$

$$= 263.404 - (123.939 \cdot 10^{-2})\,\tilde{\mathrm{Re}}_{\theta t} + (194.548 \cdot 10^{-5})\,\tilde{\mathrm{Re}}_{\theta t}^{2} - (101.695 \cdot 10^{-8})\,\tilde{\mathrm{Re}}_{\theta t}^{3} \quad \text{if } 400 \ge \tilde{\mathrm{Re}}_{\theta t} < 596$$

$$= 0.5 - 3.0 \cdot 10^{-4}(\tilde{\mathrm{Re}}_{\theta t} - 596.0) \quad \text{if } 596 \ge \tilde{\mathrm{Re}}_{\theta t} < 1200$$

$$= 0.3188 \quad \text{if } 1200 \ge \tilde{\mathrm{Re}}_{\theta t} \qquad (13)$$

The boundary conditions for the intermittency factor γ at free-stream, flow outlet and walls are set to zero flux. At inlet, γ=1 is applied. For the scalar $Re_{\theta t}$ the boundary conditions were set to zero flux at free-stream, flow outlet and walls. The boundary conditions for the scalar $Re_{\theta t}$ at an inlet should be calculated from empirical correlations based on the inlet turbulence intensity.

Before Menter *et al.* (2009) provided the empirical correlations, a number of researchers have tried to identify those functions and proposed their correlations based on flat plate experiments. In this paper, we have selected the correlations developed from Toyoda *et al.* (2007) and Kelterer *et al.* (2010).

In order to close the transition model, Toyoda *et al.* (2007) employed the following correlations:

$$\mathrm{Re}_{\theta c} = 0.9\tilde{\mathrm{Re}}_{\theta t} \qquad (14)$$

$$\mathrm{Re}_{\theta t} = [110.0 + e^{(7.08 - Tu)}]F(\lambda_{\theta}, K) \qquad (15)$$

where $F(\lambda_\theta,K)$ is a function of pressure gradient λ_θ and the acceleration parameter K and represents the effect of the pressure gradient along the streamlines. The correlation for the transition length is obtained from the correlation of the transition length Reynolds number, proposed by Mayle (1991) and is multiplied by a factor of 10,

$$F_{length} = 1260\tilde{\mathrm{Re}}_{\theta t}^{1.4} \qquad (16)$$

Based on the results derived from their flat plate experiments, Kelterer *et al.* (2010) proposed their own correlations for the critical and transitional momentum thickness Reynolds number:

$$\mathrm{Re}_{qt} = 803.73 \times \left(\frac{1}{(Tu + 0.6067)^{1.027}}\right) F(I_q) \qquad (17)$$

$$\mathrm{Re}_{\theta c} = 1.02 \cdot \tilde{\mathrm{Re}}_{\theta t} - 35 + 36 \cdot \tanh\left(-\left(\frac{\tilde{\mathrm{Re}}_{\theta t} - 138}{54}\right)\right) \quad \text{if } \tilde{\mathrm{Re}}_{\theta t} \le 215$$

$$= 45\tanh\left(\frac{\tilde{\mathrm{Re}}_{\theta t} - 215}{15}\right) + 155 \quad \text{if } \tilde{\mathrm{Re}}_{\theta t} > 215 \qquad (18)$$

while the empirical correlation for the F_{length} is given as:

$$F_{length} = \min[250.0 \cdot e^{\left[-\left(\frac{\tilde{\mathrm{Re}}_{\theta t}}{130}\right)\right]^{1.7}} + 10; 40] \qquad (19)$$

Lately, Menter *et al* (2015) developed a simplified version of the κ-ω–γ-$Re_{\theta t}$ model. The main goal was to avoid the transport equation for $Re_{\theta t}$ by evaluating the correlation inside the boundary layer and not outside. This way, he managed to achieve a Galilean formulation and simplified drastically the initial κ-ω–γ-$Re_{\theta t}$ model by reducing the formulation to only one additional equation.

The form for the transport equation for the intermittency γ has formally not been changed from the one given in the κ-ω–γ-$Re_{\theta t}$ model (equation 9). The transition source term has been slightly simplified and is now defined as:

$$P_\gamma = F_{length}\,\rho S\gamma(1-\gamma)F_{onset} \tag{20}$$

where S is the strain rate magnitude. The term, which is equal to zero upstream of the transition point, is controlled from the function F_{length} which is a constant to this model. The destruction/relaminarization source is identical to the one used in the κ-ω–γ-$Re_{\theta t}$ model.

The formulation for the F_{onset} function, which is used to trigger the intermittency production is similar to the initial model and is based on the ration of the local vorticity Reynolds number Re_V to the critical Reynolds number $Re_{\theta c}$. However, the $Re_{\theta c}$ is not computed from a transport equation but algebraically, using k and other local variables. The formulation for the current model is:

$$\mathrm{Re}_{\theta c} = C_{Tu1} + C_{Tu2}e^{\left[-C_{Tu3}\cdot Tu\cdot F_{PG}(\lambda_\theta)\right]} \tag{21}$$

where C_{Tu1} defines the minimal value of the critical $Re_{\theta c}$ number. The sum C_{Tu1}+C_{Tu2} defines the maximum value for low Tu levels, while C_{Tu3} controls how fast $Re_{\theta c}$ decreases as the turbulence intensity Tu increases. For zero pressure gradient flows, the formulation of $Re_{\theta c}$ is similar to the proposed one from Abu-Ghannam and Shaw.

The function $F_{PG}(\lambda_\theta)$ is introduced to sensitize the transition onset to the streamwise pressure gradient. This function is purely empirical and is calibrated using the Falkner-Skan series of profiles. The formula for the $F_{PG}(\lambda_\theta)$ in the correlation of $Re_{\theta c}$ is defined as:

$$F_{PG}(\lambda_\theta) = \begin{cases} \min\left(1 + C_{PG1}\lambda_\theta, C_{PG1}^{\lim}\right), \lambda_\theta \geq 0 \\ \min\left(1 + C_{PG2}\lambda_\theta + C_{PG3}\min\left[\lambda_\theta + 0.0681, 0\right]\right), \lambda_\theta < 0 \end{cases} \tag{22}$$

where the constant C_{PG1} controls the value for the critical $Re_{\theta c}$ number in areas with favourable gradient, C_{PG2} with adverse pressure gradient and C_{PG3} becomes active in regions with separation, allowing correcting the $Re_{\theta c}$ value where is necessary. A limiter is applied to exclude negative values for the F_{PG} function.

The main change from the κ-ω–γ-$Re_{\theta t}$ model is that the arguments Tu and λ_θ entering the correlation $Re_{\theta c}$ are approximated locally. This removes the need for the second transport equation for Re_θ and renders the model formulation Galilean invariant. The equation for the turbulence intensity level Tu is expressed as:

$$Tu = \min\left(100\frac{\sqrt{2k/3}}{\omega d_{\omega}},100\right) \quad (23)$$

where d_{ω} is the wall distance while the product ωd_w provides a velocity scale inside the boundary layer replacing the freestream velocity U used in the κ-ω–γ-$Re_{\theta t}$ model.

The pressure gradient parameter λ_{θ} is selected in such way that in the middle of the boundary layer it is approximately equal to the pressure gradient parameter for Falkner-Skan profiles. The formula for the λ_{θ} is given by:

$$\lambda_{\theta} = -7.53\cdot 10^{-3}\frac{dV}{dy}\frac{d_{\omega}^2}{\nu} + 0.0128 \quad (24)$$

where the constants 0.0128 accounts for the case where the $dV/d\nu$ is not zero in the middle of the boundary layer for zero pressure gradient flows, due to the growth of it.

The coupling of the model with the SST turbulent model is the same as at the κ-ω–γ-$Re_{\theta t}$ model. The only modification is the introduction of an extra production term $P_k^{\lim}$ at the k-equation in to ensure the proper generation of k at the transition points of low Tu levels. This term is designed to turn itself off when the transition process is completed and the boundary layer has reached the fully turbulent state. The expression for the $P_k^{\lim}$ reads as:

$$P_k^{\lim} = 5C_k \max(\gamma - 0.2,0)\cdot(1-\gamma)\cdot F_{on}^{\lim}\cdot\max(3C_{SEP}\mu - \mu_t,0)S\cdot\Omega \quad (25)$$

$$F_{on}^{\lim} = \min\left(\max\left(\frac{\mathrm{Re}_V}{2.2\cdot\mathrm{Re}_{\theta c}^{\lim}} - 1,0\right),3\right) \quad (26)$$

where the term $\mathrm{Re}_{\theta c}^{\lim}(=1100.0)$ ensures that the term is active only for high Reynolds numbers and for separated flows. The part $\max(\gamma - 0.2,0)$ at the expression of the $P_k^{\lim}$ ensures that the whole term is activated only once the transition model is triggered and intermittency has reached a value of 0.2. The part $\max(3C_{SEP}\mu - \mu_t,0)$ switches off the additional source term at fully turbulent regions.

Results and Discussion

The flow around the V2C aerofoil designed by Dassault Aviation (DAAV) for the TFAST project was used for the computations. This aerofoil is supercritical and designed to guarantee laminarity from the leading edge till the shock location.

Care has been taken in the construction of the grid around the V2C aerofoil. The domain extends 50 chords upstream of the leading edge and downstream of the trailing edge. In the cross-stream direction, 50 chord lengths above and below

the aerofoil were used. The grid has 480 points around the aerofoil distributed equally along the upper and the lower surfaces. The wake was covered with 60 nodes while normal to wall 90 points were used with an exponential. The first cell height above the wall was $1x10^{-6}$ of the aerofoil chord.

Initially, the HMB2 solver was compared with XFOIL. The latter is a well-known tool for aerofoil aerodynamics and uses the e^N method for transition prediction. The calculations with the HMB2 solver were conducted using either the empirical transition correlations of Michel (1951) and Cebeci-Smith (1974) or the κ-ω–γ-$Re_{\theta t}$ transition model (2009). The results are for a range of incidence angles while a Mach number of 0.2 and a chord Reynolds number of $3.240x10^6$ were considered. In all cases, the free-stream turbulence intensity was fixed at 0.5%. The instantaneous pressure and skin friction coefficients for the aerofoil at an angle of attack at 6 degrees can be seen in Figures 2a and 2b. All cases show similar results for the surface pressure coefficient. While the models indicate close onset of transition, the κ-ω–γ-$Re_{\theta t}$ transition models with the correlations from Langtry and Toyoda demonstrate more sensitivity especially close to the trailing edge of the aerofoil. On the other hand, when the Kelterer's functions were used in the κ-ω–γ-$Re_{\theta t}$ transition model, the results agreed better with the results from the XFOIL code.

Figure 2 Instantaneous pressure (a) and skin friction on the upper surface (b) coefficients, Mach=0.2, Re=$3.24x10^6$, a=6deg, Tu(%)=0.5.

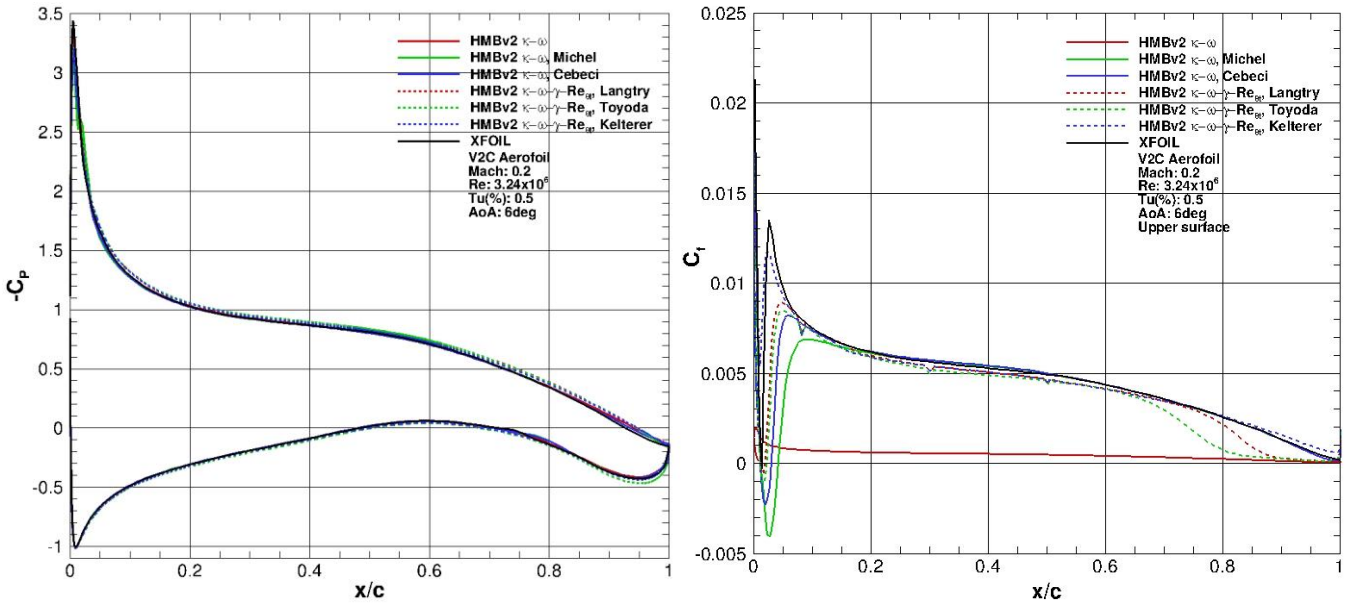

(a) (b)

For the estimation of the buffet, a Mach number of 0.7 was considered, while the chord Reynolds number and turbulence intensity remained the same, at 3.240×10^6 and 0.5%, respectively. The buffet boundary as a function of Mach number and angle of attack using the κ-ω–γ-$Re_{\theta t}$ transition model can be seen in Figure 3. At each incidence where buffet was observed, the frequency of the shock oscillations is given in Hertz. The frequency remains constant as the incidence angles increases and the Mach number remains the same, while there is an increase in buffet frequency as the Mach number increases. Figures 4a and 4b present the instantaneous pressure and skin friction coefficients for the aerofoil. The skin friction is plotted on the upper surface and the results are for the most upstream and downstream locations of the shock. At table 1, the onset of transition along with the location of the shock wave at the upper surface of the aerofoil is presented at each instance. At the specific conditions the fully turbulent calculations indicate a non-moving shock upstream from the location of the shock observed with the use of the κ-ω–γ-$Re_{\theta t}$ transition model. The use also of the 1-equation κ-ω–γ-$Re_{\theta t}$ transition model indicates also an earlier transition onset in comparison with the two-equation κ-ω–γ-$Re_{\theta t}$ transition model.

The time averaged pressure coefficient is shown in Figure 5. The suction side is composed of three main parts, the supersonic plateau (0<x/c<0.5), the spread compression due to the unsteady shock wave and the recompression zone. The pressure side is characterised by rear loading caused due to the specific aerofoil shape.

Figure 3 Region of shock oscillation for the V2C aerofoil using the κ-ω–γ-$Re_{\theta t}$ model.

The frequencies indicated in brackets are at Hz

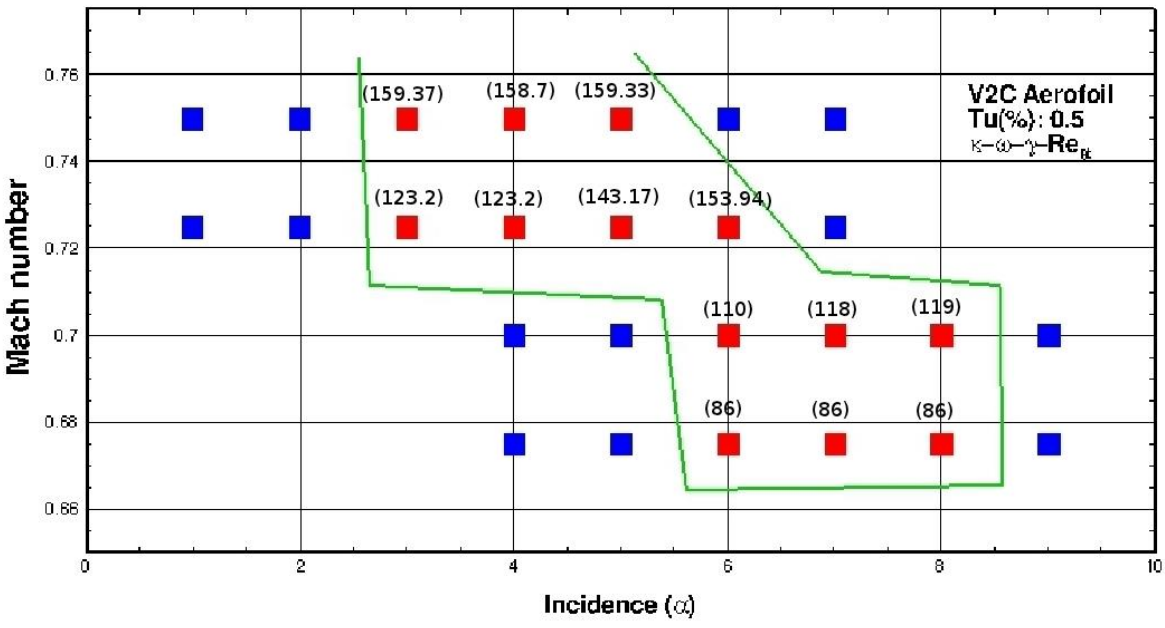

Figure 4 Instantaneous pressure (a) and skin friction on the upper surface (b) coefficients, Mach=0.7, Re=3.24x10^6, a=6deg, Tu(%)=0.5

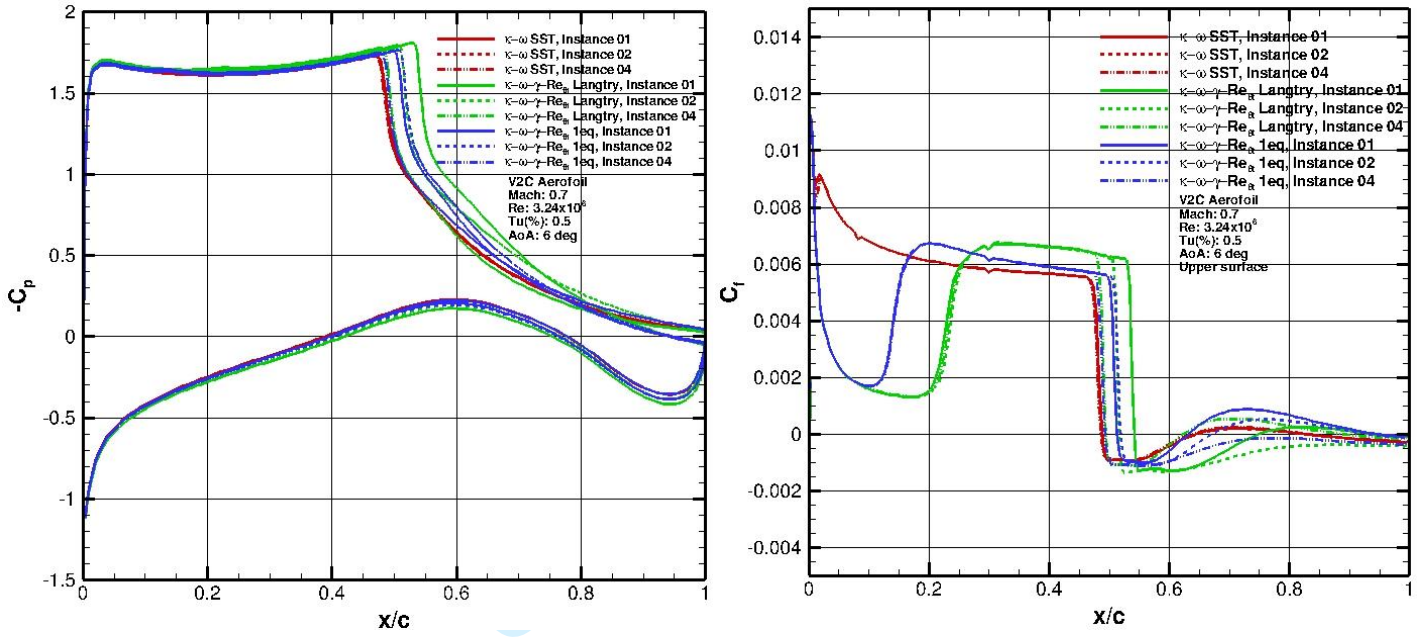

(a) (b)

Figure 5 Time-averaged pressure (a) and skin friction on the upper surface (b) coefficients, Mach=0.7, Re=3.24x10^6, a=6deg, Tu(%)=0.5

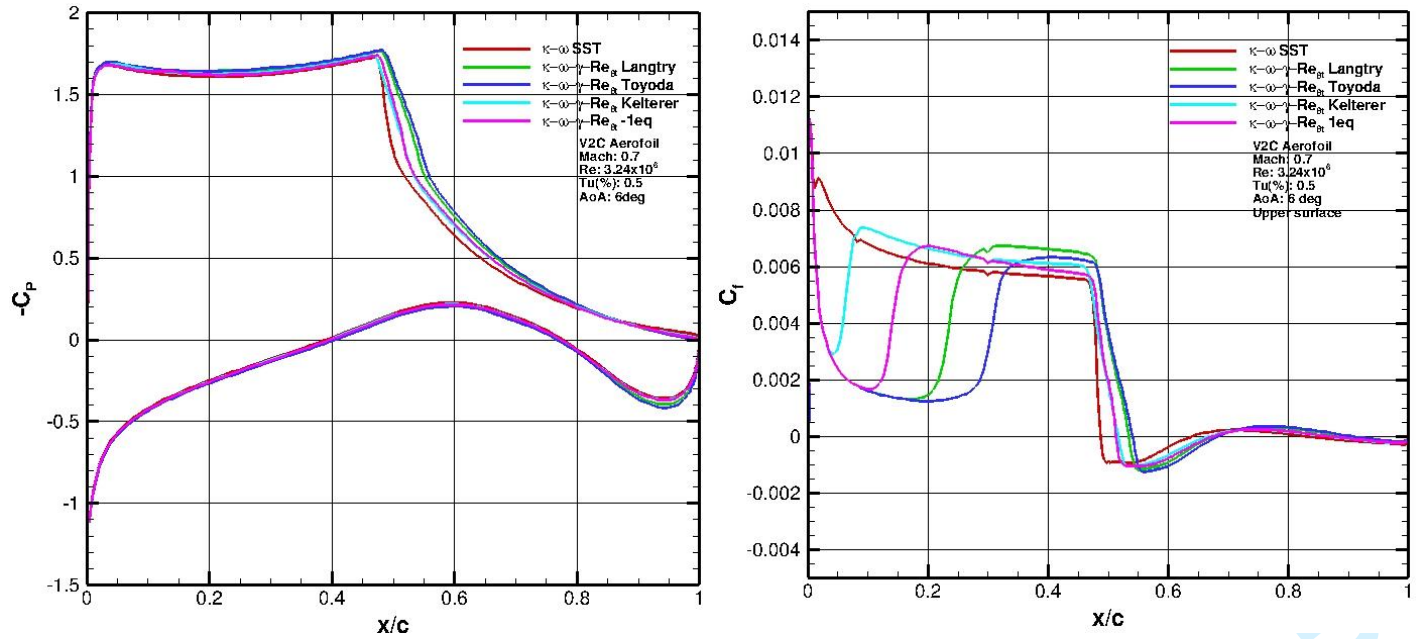

(a) (b)

Table 1. Transition point (TP) and shock wave locations (SW) on the upper surface of V2C aerofoil for different instances, Mach=0.7, Re=3.24x10^6, a=6deg, Tu(%)=0.5

Instance	Fully Turbulent		κ-ω–γ-Re$_{\theta t}$		κ-ω–γ-Re$_{\theta t}$ Toyoda		κ-ω–γ-Re$_{\theta t}$ Kelterer		κ-ω–γ-Re$_{\theta t}$ 1 Equation	
	TP	SW	TP	SW	TP	SW	TP	SW	TP	SW
1	-	0.483	0.228	0.537	0.299	0.542	0.065	0.522	0.141	0.508
2	-	0.483	0.232	0.488	0.301	0.488	0.065	0.493	0.141	0.507
3	-	0.483	0.232	0.491	0.306	0.497	0.065	0.473	0.141	0.488
4	-	0.483	0.232	0.501	0.307	0.516	0.065	0.476	0.141	0.481
5	-	0.483	0.232	0.531	0.305	0.542	0.065	0.493	0.141	0.483
6	-	0.483	0.232	0.542	0.3	0.548	0.065	0.514	0.141	0.495

Figure 6 History of the lift (a) and drag (b) coefficients, Mach=0.7, Re=3.24x106, a=6deg, Tu(%)=0.5

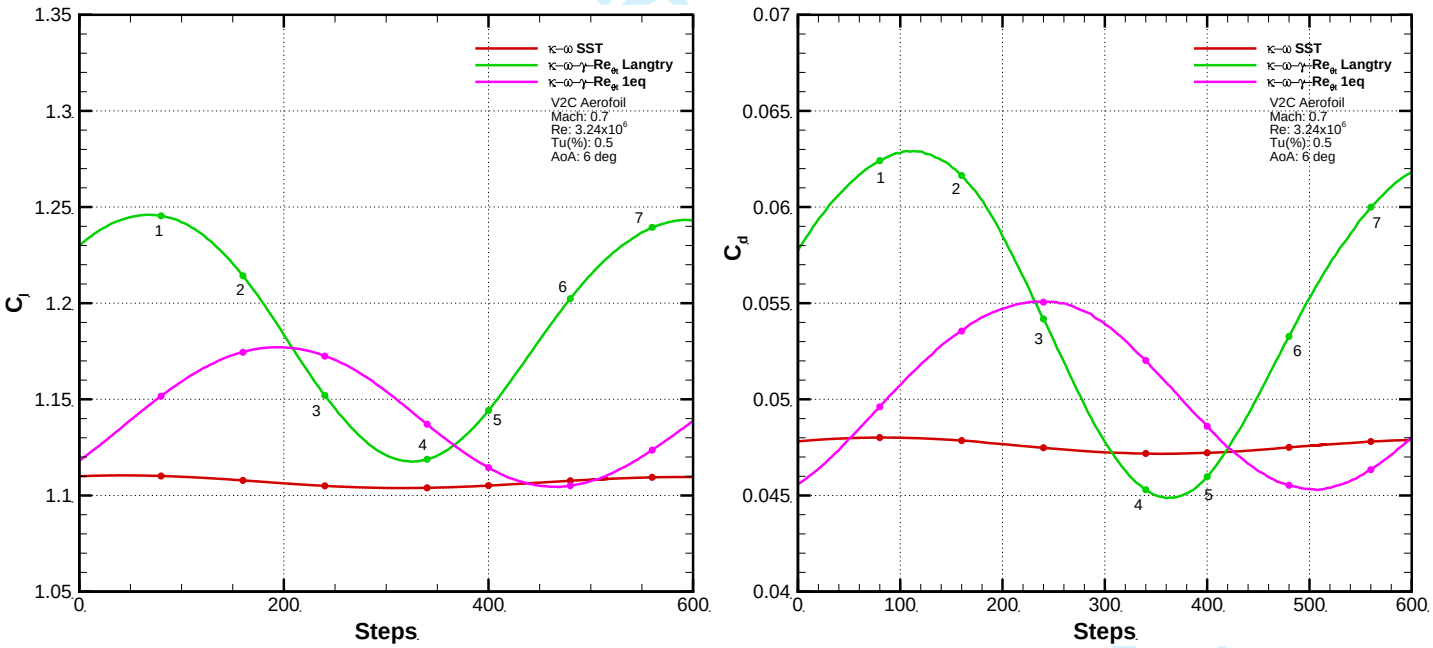

(a) (b)

The time history of the lift coefficient is shown in Figure 6a. The shock motion causes the low-frequency cycles. During a cycle, six instances are picked and shown in Figure 7. A bubble is created at the foot of the shock (instance 1). The separated flow begins to grow downstream as buffet becomes more severe until the flow is completely separated. On the other hand, the trailing edge separation moves upstream until it reaches the shock wave. Eventually the two separated

regions merge (instance 4). During this cycle, the shock wave periodically moves downstream and upstream with variable strength. As shown in Figure 6, the shock wave begins to move downstream from instance 4 (most upstream location) while at instance 1 (the most downstream location), both the shock wave and the separation point move upstream. It is also noticed that the height of the separated flow layer behind the shock wave is higher for stages 1 till 3 than for stages 4 to 6.

The difference between the two transition models from Menter is demonstrated in figure 8. The location of the shock wave at the most upstream and downstream is presented for the upper surface for the V2C aerofoil. The κ-ω–γ-$Re_{\theta t}$ transition model indicates the existence of a larger separation bubble at the foot of the shock wave in comparison to the 1-equation LCTM transition model.

Figure 7 Mach number coefficient during one buffet cycle,

Mach=0.7, Re=3.24x10^6, a=6deg, Tu(%)=0.5, κ-ω–γ-$Re_{\theta t}$.

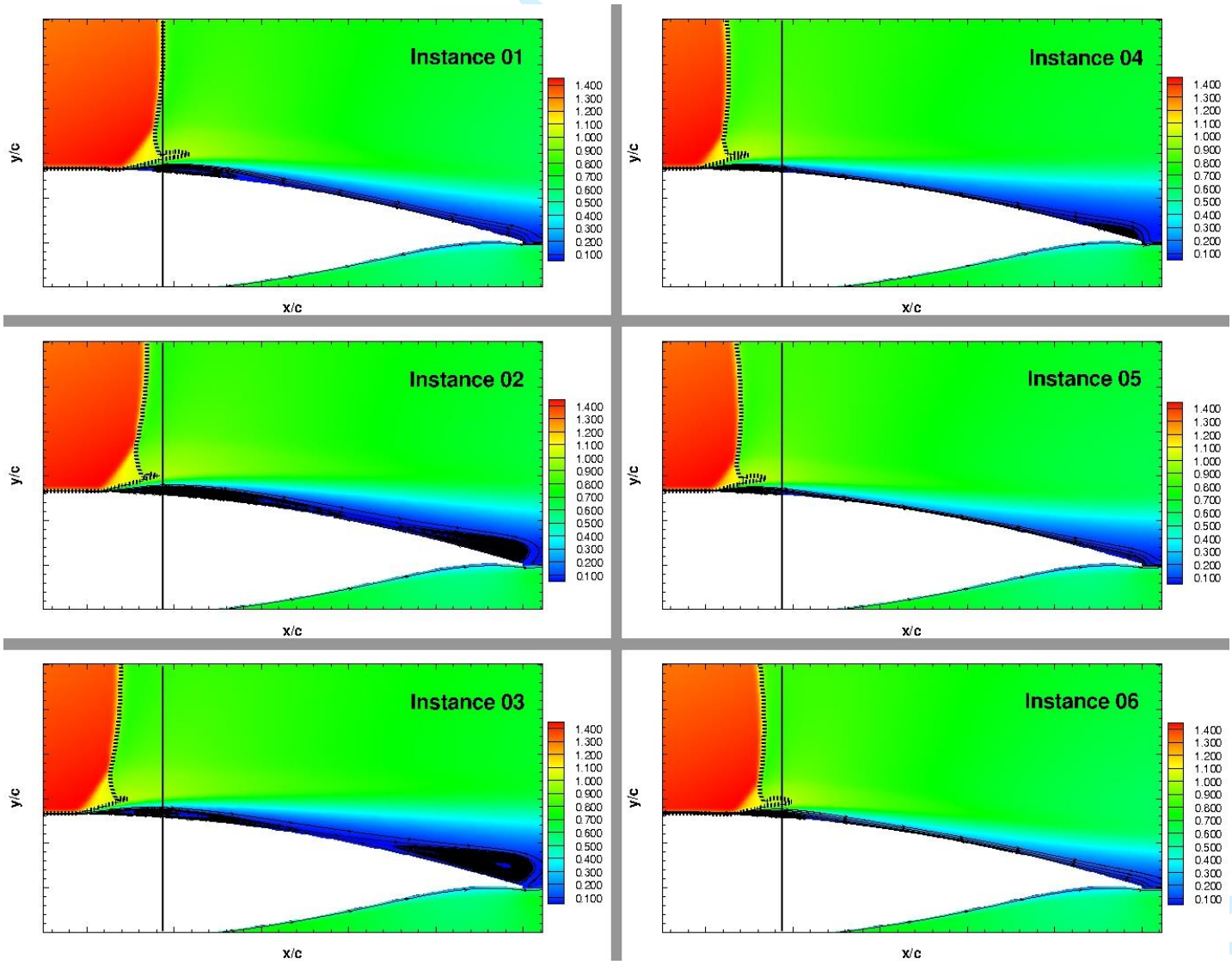

Figure 8 Mach number coefficient at the most upstream, and downstream, location during κ-ω–γ-$Re_{\theta t}$ and κ-ω–γ calculations, Mach=0.7, Re=3.24x10^6, a=6deg, Tu(%)=0.5

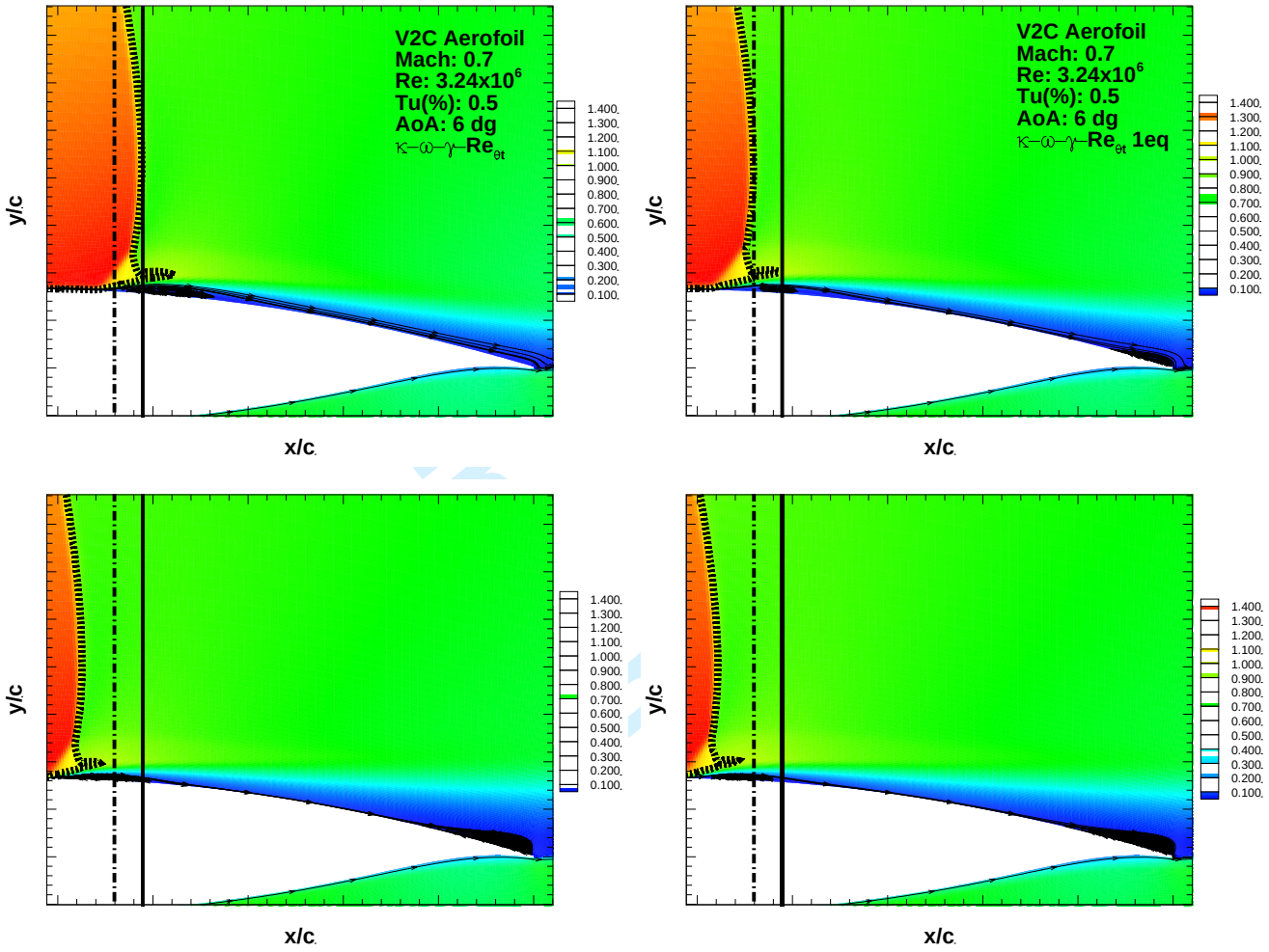

DAAV also provided the geometry of a 3D laminar wing for the TFAST project. The goal was to understand the transition effect on wing buffet. The wing was based on the aforementioned V2C aerofoil, had aspect ratio of 8 and a leading edge sweep angle of 20 degrees.

Following the same procedure for the construction of the grid around the wing as followed for the V2C aerofoil case, the domain extended 50 chords upstream of the leading edge and downstream of the trailing edge. In the cross-stream direction, 50 chord lengths above and below the wing were used. The height for the first cell above the wall was 1x10^{-6} of the wing rot chord.

The calculations were performed at conditions similar to the 2D aerofoil with the Reynolds and Mach numbers at 4.4x10^6 and 0.7821, respectively. The turbulence intensity was fixed at 2.58% and the incidence angle at 7 degrees. The time history of the lift coefficient is shown in Figure 8a. The frequency for the buffet was 14.74Hz. The instantaneous pressure and skin friction coefficients at the mid-span of the wing during a cycle can be seen in Figures 9a and 9b. The skin friction

is given for the suction side of the wing and the results show the movement of the shock from the most upstream to the most downstream location.

Even if the frequency of buffet is lower in comparison to the frequencies observed during the 2D aerofoil computations, due to longer chord of the wing and higher Mach number of the test case, the Strouhal number (St) for the wing is comparable to the results from the 2D aerofoil at Re=3.240x10^6 and Mach=0.7. During a buffet cycle, similar phenomena like for the 2D aerofoil were observed.

Figure 9 History of lift (a) and drag (b) coefficients versus time,

Mach=0.7821, Re=4.4x10^6, a=7deg, Tu(%)=2.58, κ-ω–γ-$Re_{\theta t}$.

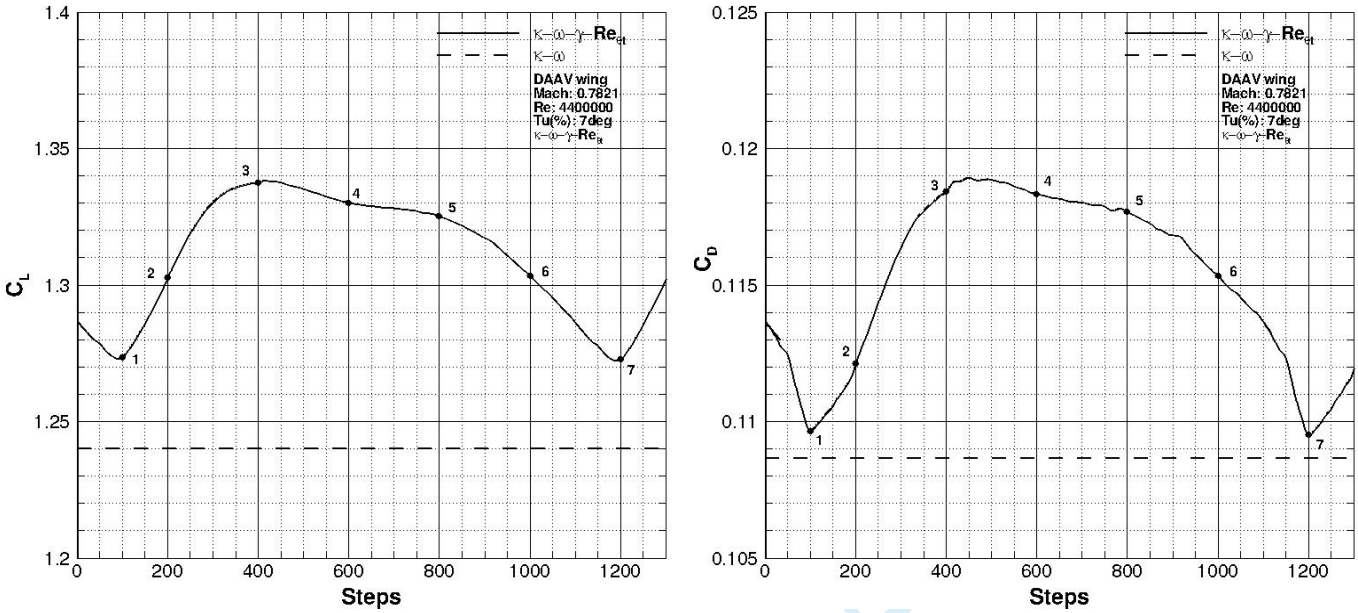

(a) (b)

Hence, during a cycle, the shock wave developed on the upper surface moved periodically downstream and upstream with the developed separation bubble at the foot of the shock changed in size and merged with the trailing edge separation. The Mach number visualisation of the flow during six instances of a cycle at the middle of the wing can be seen in Figure 10.

Figure 10 Instantaneous pressure (a) and skin friction on the upper surface

(b) coefficients at the mid-span of the wing,

Mach=0.7821, Re=4.4x10^6, a=7deg, Tu(%)=2.58, κ-ω–γ-Re$_{θt}$.

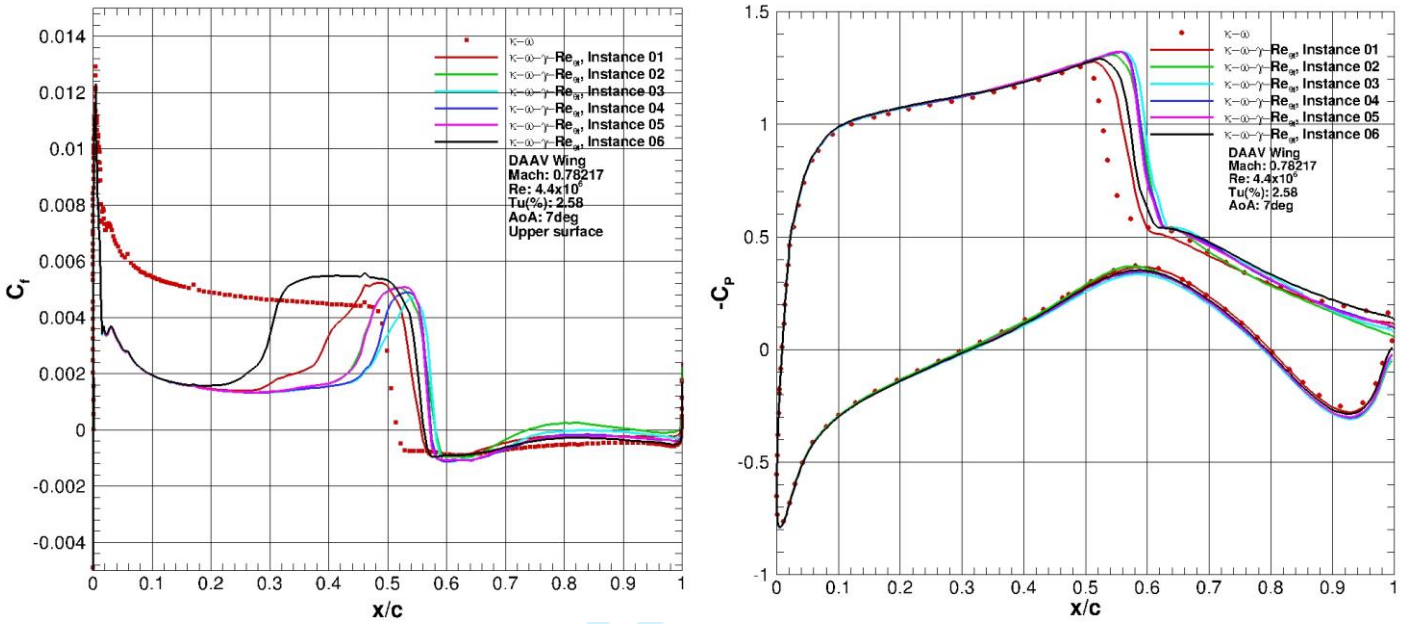

(a) (b)

Conclusions and Future Work

The obtained results for the transitional SWBLI are encouraging and suggest that buffet may also be encountered for the transitional SWBLI case. The results from the different variations of the κ-ω–γ-Re$_{θt}$ model suggested that the model is sensitive on the correlations that closure the model. The 2D and 3D cases were driven by a similar flow mechanism and buffet occurred at similar Strouhal numbers.

At this stage of the work there are no direct comparisons against experiments though this situation will change with progress in the TFAST project. It is anticipated that the available experimental data will include not only flow visualisation but also detailed measurements of unsteady pressure that will allow for the detailed validation of CFD methods and turbulence closures for this very interesting flow case. Further computations with flow control and different transition correlations are also planned.

Acknowledgments

This work is supported by the EU Collaborative Project TFAST, FP7-AAT-2010-RDT-1, under Grant Agreement N°265455.

Figure 11 Mach number visualisation during one buffet cycle on the mid-span of the wing, Mach=0.7821, Re=4.4x10^6, a=7deg, Tu(%)=2.58, κ-ω–γ-Re$_{\theta t}$.

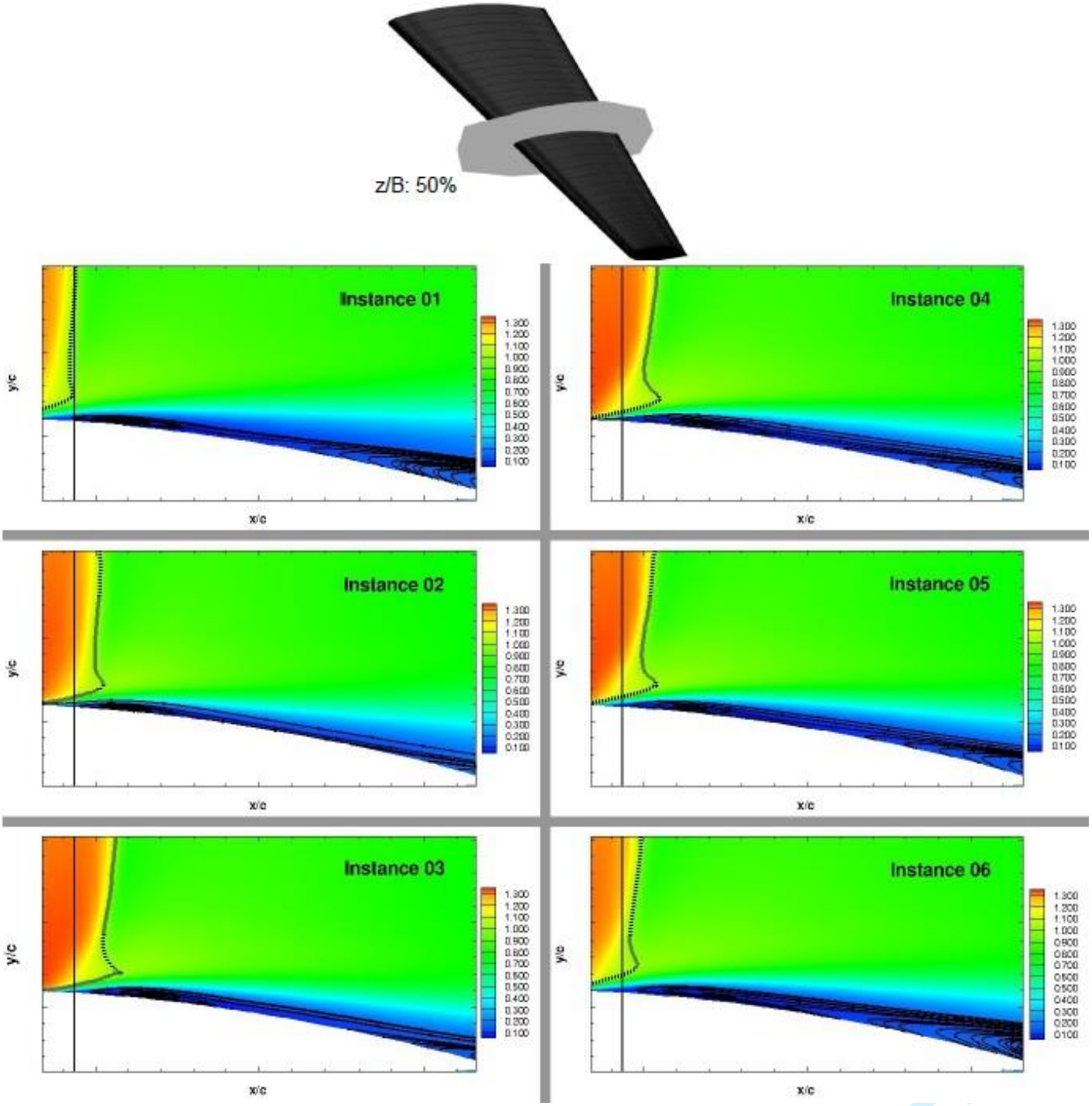

References

Abu-Ghannam, B.J. and Shaw, R., (1980). “Natural Transition of Boundary Layer – The effect of Turbulence”, Pressure Gradient and Flow Flow History, *Journal of Mechanical Engineering Science*, 22:5.

Axelsson, O. (1994), “Iterative Solution Methods”, Cambridge University Press, Cambridge, MA.

Barakos, G. and Drikakis, D., (2000). “Numerical simulations of transonic buffet flows using various turbulence closures”, *International Journal of Heat and Fluid Flows,* **21**:620-626.

Boin, J.-Ph., Robinet, J.-Ch. Corre C., and Deniau, H. (2006). "3D steady and unsteady bifurcations in a shock-wave/laminar boundary layer interaction: a numerical study", Theoretical and Computational Fluid Dynamics, **20**(3):163-180.

Cebeci, T. and Smith, A.M.O, (1974). *Analysis of Turbulent Boundary Layers*, Academic Press.

Cho, J.R. and Chung, M., (1992). “A $\kappa-\varepsilon-\gamma$ equation turbulence model”, *Journal of Fluid Mechanics*, **237**:301-322.

Deck, S. (2005), “Numerical Simulation of Transonic Buffet over a Supercritical Airfoil”, AIAA Journal, Vol. 43, **7**:1556-1566.

Dhawan, S. and Narasihma, R., (1958). “Some properties of boundary layer flow during the transition from laminar to turbulent motion”, *Journal of Fluid Mechanics*, **4**:418-436.

Grossi, F., Braza, M. and Hoarau, Y. (2014), “Delayed Detached-Eddy Simulation of the Transonic Flow around a Supercritical Airfoil in the Buffet Regime”, *Progress in Hybrid RANS-LES Modelling*, **117**:369-378.

Iovnovich, M. and Raveh, D.E., (2011), “Reynolds-Averaged Navier-Stokes study of the Shock-Buffet instability mechanism”, AIAA Journal, Vol. 50, **4**:880-890.

Iovnovich, M. and Raveh, D.E., (2014), “Numerical study of Shock Buffet on Three-Dimensional Wings”, AIAA Journal, Vol. 53, **2**:449-463.

Jacquin, L., Molton, P., Deck, S., Maury, B. and Soulevant, D., (2009), “Experimental study of shock oscillation over a transonic supercritical profile”, AIAA Journal, Vol. 47, **9**:1985-1994

Jameson, A. (1991). “Time Dependent Calculations using Multigrid, with Applications to Unsteady Flows Past Airfoils and Wings”, 10th Computational Fluid Dynamics Conference, Honolulu, HI, AIAA-91-1596.

Kelterer, M.E., Pecnik, R., and Sanz, W., 2010. “Computation of Laminar-Turbulent Transition in Turbomachinery Using the Correlation-Based γ-$Re_{\theta t}$ Transition Model”, Proceedings of ASME Turbo Expo 2010: Power for Land, Sea and Air, June 14-18.

Lee, B. H. K., (2001). “Self-sustained shock oscillations on airfoils at transonic speeds”, *Progress in Aerospace Sciences*, **37**:147-196.

Levy, Jr. L. L., (1978). “Experimental and Computational Steady and Unsteady Transonic Flows about a Thick Aerofoil”, *AIAA Journal*, Vol.16, **6**:564-572.

Marvin, J. G. and Levy, Jr. L. L., Seegmiller, H. L., (1980). ”Turbulence Modeling of Unsteady Transonic Flows”, *AIAA Journal*, Vol. 18, **5**:489-496.

Mayle, R.E., (1991). ”The Role of Laminar-Turbulent Transition in Gas Turbine engine”, *ASME Journal of Turbomachinery*, Vol. 113, p. 509-537.

McDevitt, J. B. and Levy, Jr. L. L., Deiwert, G. S., (1976). ”Transonic Flow About a Thick Circular-Arc Airfoil”, *AIAA Journal*, Vol. 14, **5**:606-613.

McDevitt, J. B. and Okuno, A. F., (1985). Static and Dynamic Pressure Measurements on a NACA 0012 Airfoil in the Ames High Reynolds Number Facilitiy, NASA TP, NASA.

Michel, R. (1951). Etude de la Transition sur les Profils d’Aile, Etablissement d’um Critere de Determination du Point de Trasition et Calcul de la Trainee de Profil Incompressible, ONERA.

Menter, F.R. and Langtry, R.B., (2009). ”Correlation-Based Transition Modelling for Unstructured Parallelized Computational Fluid Dynamics Codes”, *AIAA Journal*. **47**:2894-2906

Menter, F.R., Smirnov, P.E.. Liu, T. and Avancha,R., (2015). ”A One-Equation Local Correlation-Based Transition Model”, Springer, Flow, Turbulence and Combustion.

Menter, F.R. and Egorov, Y., (2005). “A Scale-Adaptive Simulation Model using Two-equation Models”, 43rd AIAA Aerospace Sciences Meeting and Exhibit, 10-13 January 2005, Reno, Nevada.

Osher, S. and Chakravarthy, S., (1983). “Upwind schemes and boundary layer conditions with applications to Euler equations in general geometries”, *Journal of Computational Physics*, **50**:447-481.

Raveh, D., (2009), “A numerical study of an oscillating airfoil in transonic buffeting flows”, AIAA Journal, Vol. 47, **3**:505-515.

Savill, A.M., (1993). “Some Recent Progress in the Turbulence Modeling of By-Pass Transition, Near-Wall Turbulent Flows”, edited by R.M.C. So, C.G. Speziale, and B.E. Launder, Elsevier, New York, p. 829.

Seegmiller, H. L.and Marvin, J. G., Levy, Jr. L. L., (1978). “Steady and Unsteady Transonic Flow”, *AIAA Journal*, **16** (12):1262-1270.

Shur, M., Spalart, P.R., Strelets, M. and Travin A., (1999). “Detached-Eddy Simulation of an Airfoil at High Angle of Attack”. 4th Int. Symposium on Eng. Turb. Modeling and Experiments, May 1999, Corsica, France.

Steelant, J. and Dick, E., (1996). “Modelling of bypass transition with conditioned Navier-Stokes equations coupled to an intermittency transport equation”, *International Journal for Numerical Methods in Fluids*, Vol:23, **3**:193-220.

Suzen, Y.B. and Huang, P.G., (1999). “Modelling of flow transition using an intermittency transport equation”, Technical Report NASA/CR-1999-209313.

Thiery, M. and Coustols, E., (2005). “URANS computations of shock-induced oscillations over 2-D rigid airfoils: Influence of test section geometry”, *Flow, Turbulence and Combustion*, **74**:331-354.

Tijdeman, H. and Seebass, R., (1980). “Transonic flow past oscillating airfoils”, *Annu Rev Fluid Mech*, **12**:942-944.

Toyoda, A., Misaka, T., and Obayashi, S., (2007). “An Application of Local Correlation-Based Transition Model to JAXA High-Lift Configuration Model”, *25th AIAA Applied Aerodynamics Conference*, Vol. 2, p.1390-1400.

van Leer B., (1979). “Towards the ultimate conservative study of computational methods in cosmic gas dynamics”. Journal of Computational Physics, **32**:101-136.

van Albada G.D. and van Leer, B., Roberts, W.W., (1982). “A comparative study of computational methods in cosmic gas dynamics”, Astronomy & Astrophysics, **108**:76-84.

Nomenclature

Symbols

c	Aerofoil chord
F_{length}	Function for the length at κ-ω–γ-$Re_{\theta t}$ model
i,j,k	Spatial components
M	Mach number
R	Cell conserved residuals
Re	Reynolds number based on the chord
$Re_{\theta c}$	Critical momentum thickness Reynolds number
$Re_{\theta,s}$	Momentum thickness Reynolds number at start
$Re_{\theta,\varepsilon}$	Momentum thickness Reynolds number at end
$Re_{\theta,tr}$	Momentum thickness Reynolds number at transition point
$Re_{x,tr}$	Reynolds number at transition point based on the distance from the leading edge of the aerofoil
St	Stouhal number
Tu	Turbulence intensity
γ	Intermittency
κ	Kinetic energy of turbulence
λ_θ	Pressure gradient parameter
ω	Turbulence frequency

Definitions, Acronyms and Abbreviations

BILU	Block Incomplete Lower-Upper preconditioner
CFD	Computational Fluid Dynamics
DAAV	Dassault Aviation
DES	Detached Eddy Simulation
ERCOFTAC	European Research Community on Flow Turbulence and Combustion
GCG	Genelarised Conjugated Gradient
HMBv2	Helicopter Multi-Block solver

IDDES Improved Detached Eddy Simulation

LES Large Eddy Simulation

LCTM Local Correlation-Based Model

MUSCL Monotone Upstream-Centre Scheme for Conservation Laws

SWBLI Shock wave –Boundary layer Interaction

RANS Reynolds-Averaged Navier-Stokes

SAS Scale-Adaptive Simulation

URANS Unsteady Reynolds-Averaged Navier-Stokes

Manuscript ID AEAT-05-2015-0123
"Implicit CFD Methods for Transitional Shock Wave – Boundary Layer Interaction"
Aircraft Engineering and Aerospace Technology

The reviewer suggest the authors improve the paper in the following aspects:

(1) More recent papers on the transition models should be discussed and compared.
The introduction is now revised to include more papers on the topic.

(2) Instead of introducing very basic CFD theories and transition models, the authors should pay more effort on the implementation of the transitions models in the CFD solver.
This is now done, the details of the implicit scheme in HMB are now presented.

(3) As the authors stated themselves, the results would be more convincing if compared with the experimental results.
Unfortunately this is not possible at the moment due to the experiments running very late in the TFAST project. We should of course re-visit this once test data become available.

Additional Questions:

1. Originality: Does the paper contain new and significant information adequate to justify publication?: Yes. This paper presents methods for transition prediction and some encouraging results for shock wave boundary layer interaction.

2. Relationship to Literature: Does the paper demonstrate an adequate understanding of the relevant literature in the field and cite an appropriate range of literature sources? Is any significant work ignored?: The authors reviewed previous research work on transition modeling, however, the latest publication in the recent five years are not included. See item 1 on the comments list.

3. Methodology: Is the paper's argument built on an appropriate base of theory, concepts, or other ideas? Has the research or equivalent intellectual work on which the paper is based been well designed? Are the methods employed appropriate?: The conventional CFD theories and transition models are introduced in the paper. However, the implementation of the transition models and the solution techniques are not introduced in detail. See item 2 on the comments list.

4. Results: Are results presented clearly and analysed appropriately? Do the conclusions adequately tie together the other elements of the paper?: Encouraging results are obtained using HMB2 with the transition models. The comparisons of the results of different methods are also carried out to show the effectiveness of the solver.

5. Implications for research, practice and/or society: Does the paper identify clearly any implications for research, practice and/or society? Does the paper bridge the gap between theory and practice? How can the research be used in practice (economic and commercial impact), in teaching, to influence public policy, in research (contributing to the body of knowledge)? What is the impact upon society (influencing public attitudes, affecting quality of life)? Are these implications consistent with the findings and conclusions of the paper?: The shock wave boundary layer interaction is an important concern for the aeronautical engineering. The authors implement different kinds of transition models in the CFD solver, and produce satisfactory results for this problem.

6. Quality of Communication: Does the paper clearly express its case, measured against the technical language of the field and the expected knowledge of the journal's readership? Has attention been paid to the clarity of expression and readability, such as sentence structure, jargon use, acronyms, etc.: Yes.